nature portfolio

https://doi.org/10.1038/s41558-022-01339-z

Supplementary information

Antarctic sea-ice expansion and Southern Ocean cooling linked to tropical variability

In the format provided by the authors and unedited

Supplementary Information for

Antarctic sea ice expansion and Southern Ocean cooling linked to tropical variability

Eui-Seok Chung[1], Seong-Joong Kim[1*], Axel Timmermann[2,3], Kyung-Ja Ha[2,4,5], Sang-Ki Lee[6], Malte F. Stuecker[7], Keith B. Rodgers[2,3], Sun-Seon Lee[2,3], and Lei Huang[2,3]

[1]Division of Atmospheric Sciences, Korea Polar Research Institute, Incheon, South Korea
[2]Center for Climate Physics, Institute for Basic Science, Busan, South Korea
[3]Pusan National University, Busan, South Korea
[4]Department of Climate System, Pusan National University, Busan, South Korea
[5]BK21 School of Earth and Environmental Systems, Pusan National University, Busan, South Korea
[6]Atlantic Oceanographic and Meteorological Laboratory, NOAA, Miami, FL, USA
[7]Department of Oceanography and International Pacific Research Center, School of Ocean and Earth Science and Technology,
University of Hawaiʻi at Mānoa, Honolulu, HI, USA

*e-mail: seongjkim@kopri.re.kr

Supplementary Text 1

In this study, given the quasi-oscillatory nature of internal variability, we assume that longer records with multiple independent observations give a better indication of the forced response. For instance, although the external forcing is much stronger over 1979–present than it is over 1950–present, as shown in Extended Data Fig. 2, it is possible that internal variability could obscure or offset much of the GHG-induced warming over the period 1979–present. In contrast, over 1950–2020 the GHG-induced warming signal clearly emerges from the noise of internal variability. This contrast, therefore, supports the assumption that longer observational records give a better indication of the forced response. Due to the data quality issue over the period prior to ~1979, it is possible that the inferred forced response is incorrect in sign. However, such a case can be avoided by employing multiple independent observations.

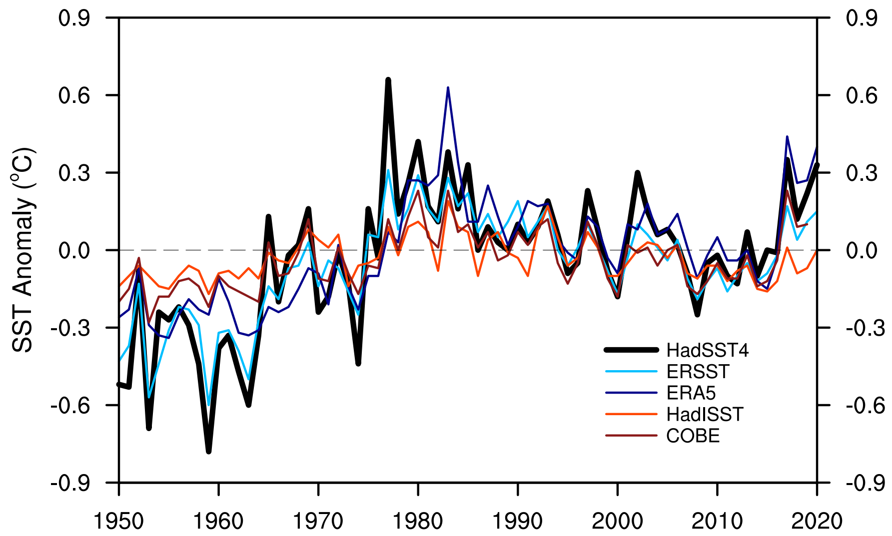

Supplementary Fig. 1: Timeseries of Southern Ocean-mean SST anomalies relative to the 1961-1990 means for non-interpolated (HadSST4) and interpolated (ERSST, ERA5, HadISST and COBE) datasets. Note that Southern Ocean-mean (south of 50°S) timeseries are constructed using SST anomalies at the grid points where HadSST4 data are available.

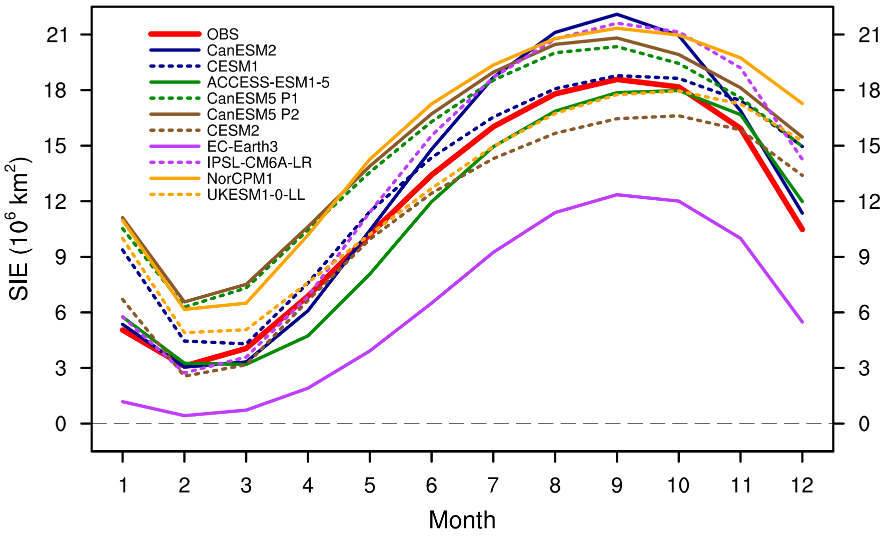

Supplementary Fig. 2: Mean seasonal cycle of Antarctic total sea ice extent over the period 1979–2014 for observations (NSIDC G02135, thick red line) and model simulations (ensemble mean for individual models).

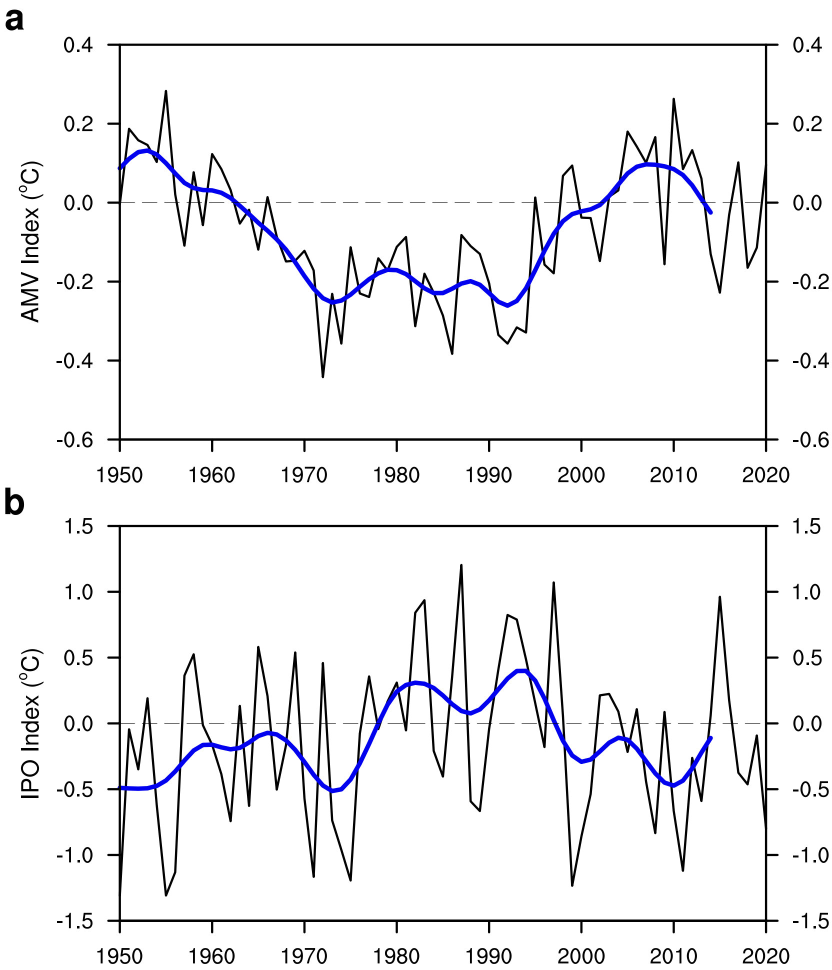

Supplementary Fig. 3: Time evolution of tropical decadal variability over 1950–2020. **a**, Timeseries of unfiltered AMV index, with low-pass filtered quantity represented by thick blue curve. **b**, Same as in **a**, but for the IPO index.

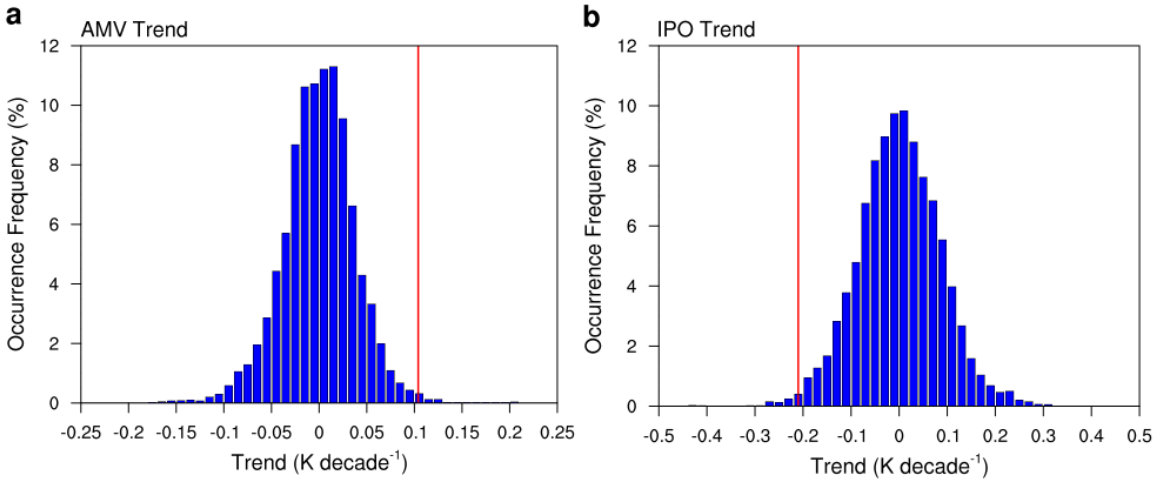

Supplementary Fig. 4: Observed AMV and IPO trends over the period 1979–2014 in the context of model-simulated probability distributions. **a**,**b**, Histograms of the AMV trends (**a**) and the IPO trends (**b**) over overlapping 36-year periods in pre-industrial control runs. The vertical lines in red denote the observed trends over the period 1979–2014.

Supplementary Table 1. List of the observational datasets analyzed in this study.

Data Set	**Variable**	**Period**
NSIDC G02135	Sea Ice Extent	1979–2020
NSIDC 0192	Sea Ice Extent	1973–2002
NSIDC G00917	Sea Ice Extent	1973–1990
Nimbus-1	Sea Ice Extent	September 1964
HadISST	Sea Ice Concentration	1979–2020
ERSSTv5	SST	1950–2020
HadISST	SST	1950–2020
COBE SST2	SST	1950–2019
ERA5	SST	1950–2020
HadCRUT5	Surface Temperature	1950–2020
GISTEMPv4	Surface Temperature	1950–2020
Berkeley Earth	Surface Temperature	1950–2020
NOAA globaltemp	Surface Temperature	1950–2020

Supplementary Table 2. Information on the model simulations analyzed in this study.

Model	Number of ensemble members	Analysis period and forcing information	Ensemble-mean trends (10^6 km^2 $decade^{-1}$ or °C $decade^{-1}$)	Length of pre-industrial control run (years)
CanESM2 Large Ensemble (M1 in Extended Data Fig. 1)	50	1950–2020 (CMIP5) Historical: 1950–2005 RCP8.5: 2006-2020	1950–1978: -0.109 (SIE) 0.017 (SST) 1979–2014: -0.423 (SIE) 0.088 (SST)	1096
CESM1 Large Ensemble (M2)	40	1950–2020 (CMIP5) Historical: 1950–2005 RCP8.5: 2006-2020	1950–1978: -0.147 (SIE) 0.027 (SST) 1979–2014: -0.431 (SIE) 0.093 (SST)	1801
ACCESS-ESM1-5 (M3)	40	1950–2014 (CMIP6) Historical: 1950–2014 SSP370: 2015–2020	1950–1978: 0.032 (SIE) 0.000 (SST) 1979–2014: -0.130 (SIE) 0.030 (SST)	900
CanESM5 (M4_1 and M4_2)	25 (physics 1) 25 (physics 2)	1950–2020 (CMIP6) Historical: 1950–2014 SSP370: 2015-2020	1950–1978: -0.139/-0.065 0.015/0.010 (SST) 1979–2014: -0.474/-0.504 0.100/0.096 (SST)	1000 (physics 1) 1000 (physics 2)
CESM2 Large Ensemble (M5)	100*	1950–2020 (CMIP6) Historical: 1950–2014 SSP370: 2015-2020	1950–1978: -0.116 (SIE) 0.016 (SST) 1979–2014: -0.393 (SIE) 0.083 (SST)	1200
EC-Earth3 (M6)	69 (1979–2014) 19 (1950–1978) 57 (1979–2020)	1950–2014 (CMIP6) Historical: 1950–2014 SSP370: 2015-2020	1950–1978: 0.040 (SIE) -0.004 (SST) 1979–2014: -0.225 (SIE) 0.068 (SST)	501
IPSL-CM6A-LR (M7)	32 (1950–2014) 11 (1979–2020)	1950–2014 (CMIP6) Historical: 1950–2014 SSP370: 2015-2020	1950–1978: 0.002 (SIE) -0.002 (SST) 1979–2014: -0.431 (SIE) 0.068 (SST)	2000
NorCPM1 (M8)	30	1950–2020 (CMIP6) Historical: 1950–2020	1950–1978: -0.123 (SIE) 0.024 (SST) 1979–2014: -0.336 (SIE) 0.074 (SST)	500
UKESM1-0-LL (M9)	17 (1950–2014) 13 (1979–2020)	1950–2014 (CMIP6) Historical: 1950–2014 SSP370: 2015-2020	1950–1978: -0.029 (SIE) -0.010 (SST) 1979–2014: -0.868 (SIE) 0.133 (SST)	1880
IPSL-CM6A-LR (Pacemaker)	10	1950–2014		

*Regarding biomass burning over the period 1990–2020, two different sets of forcing fields were used in the CESM2 Large Ensemble: while the first 50 members follow CMIP6 protocols, a smoothed version of forcing fields with a 11-year running-mean filter was applied to the second 50 members[77]. As the biomass burning forcing is mainly related to wildfires over Siberia, we assume that the response of Southern Ocean climate to biomass burning is not critically sensitive to the difference between the two sets of forcing fields.